Hindawi
Shock and Vibration
Volume 2019, Article ID 8520564, 16 pages
https://doi.org/10.1155/2019/8520564

Research Article

Vibration Characteristic of High-Voltage Tower Influenced by Adjacent Tunnel Blasting Construction

Limin Duan,[1] **Wenshuai Lin**,[1] **Jinxing Lai**,[1] **Peng Zhang**,[2] **and Yanbin Luo**[1]

[1]*School of Highway, Chang'an University, Xi'an 710064, China*
[2]*State Key Laboratory of Rail Transit Engineering Informatization, China Railway First Survey and Design Institute Group Co., Ltd., Xi'an 710043, China*

Correspondence should be addressed to Jinxing Lai; laijinxing@chd.edu.cn and Peng Zhang; 982507243@qq.com

Received 6 March 2019; Accepted 5 May 2019; Published 22 May 2019

Academic Editor: Huu-Tai Thai

The effects of tunnel blast excavation on the adjacent existing high-voltage tower are comprehensively studied for the Chashan highway tunnel project as a case study. To investigate the effect of blast-induced vibration from the tunnel on the adjacent existing tower, field tests and numerical simulations method were adopted to study the vibration velocity and vibration frequency of the existing tower. Moreover, the relationship between the transverse distance from the detonation center and the peak velocity is discussed in detail. The results showed that the peak velocity of the measuring point in tower foundation increases with the distance between the detonation center and tower foundation approaches, and the maximum velocity is appearing when detonation center is 0 m. Furthermore, the corresponding energy spectrum distributions of the existing tower under the effect of blast induced by vibration is also analyzed, and the main frequency of vertical vibration is generally higher than that of transverse vibration. On combining the peak velocity with the main frequency and the natural frequency of the tower, the safety evaluation of the blasting area is proposed, and the corresponding control measures of blasting vibration are put forward. A guideline for the blast safety zone is proposed based on vibration velocity, main frequency, and the quantity of explosive.

1. Introduction

Tunnels play an important role in the transportation infrastructure of mountain areas and bring convenience to people's lives [1–7]. In China, at present, the construction of mountain tunnels mainly adopts the drilling and blasting method which is a preferred method of rock excavation worldwide due to low initial investment, cheap explosive, and possibility to deal with different complex geologies [8–10]. Although the drilling and blasting method have been widely used in underground construction, the stability of mountain body and surrounding environment has been inevitably disturbed, and the groundwater system of the mountain has been greatly affected during blasting excavation, which could increase the risk of construction safety [11–16]. For shallow-buried tunnels, surface vibration caused by drilling and blasting is relatively large to reduce the impact of blasting on surrounding buildings, and ground vibration caused by blasting in the process of tunnel construction should be reasonably controlled. Limited by the geological condition of mountain areas and economic factors, it is difficult to build tunnel far away from high-voltage towers. Furthermore, the high-voltage tower is a high-rise structure, which is very sensitive to tilt deformation and uneven settlement of foundation, and the failure of key components will result in the collapse of the structure under vibration [17, 18]. The uneven settlement of the high-voltage tower foundation is caused by tunnel blasting, which may lead to paralysis of the power supply system, huge economic losses, and even causing serious consequences such as fire. Therefore, it is crucial to reduce the influence of blasting on the high-voltage tower and ensure that the safety of the high-voltage tower in the process of tunnel blasting excavation.

Study on the dynamic response of the high-voltage tower induced by tunnel blast excavation can be found in literature

[18–22]. For example, Moon et al. [23] studied experimentally the seismic behavior of a specific connection between the structural members of the transmission tower. Some studies [24–27] evaluated the vibration damage to transmission towers based on the finite element method. Tian et al. [28] investigated the effect of the types of connections used for the transmission cables and the effect of direction and the spatial variability of the earthquake on the seismic behavior of transmission towers. Luo et al. [29] analyzed the dynamic characteristic of the tunnel for surface explosion of 100 and 300 kg TNT charge, respectively, according to features of the Nanjing metro tunnel in sandy soil. Yu and Ding [30] studied the blasting technology of the tunnel under passing high-voltage tower. Yu et al. [31–33] investigated the response of the immersed tunnel under nonuniform seismic excitation, and the multipoint shaking table tests were conducted to simulate the superlong immersed tunnel.

In order to study the response of the existing building under the tunnel excavation, Zhang et al. [34] taking the Tianjin metro line 6 through the tower as the engineering background, the simulation analysis of the tower under the subway double-line tunnel is carried out by using numerical simulation. It was shown that the tower was most affected by the tunnel center within the range of 2 times the tunnel diameter. Mair et al. [35] studied the effect of tunneling on the Waterloo and City Line (WCL) tunnels, the Victory Arch, and Elizabeth House, beneath which are passed by the new tunnels. Guan [36] studied the relationship between the peak velocity of adjacent buildings and the main frequency of blasting and the natural frequency of buildings and evaluated the safety of ground.

However, as a complex, continuous, mechanical system, vibration design of the high-voltage tower system remains one of the most challenging tasks in the civil engineering design community [37]. There are still many problems to be studied about the blasting construction scheme, vibration characteristics, and safety evaluation method when the tunnel passes through the adjacent high-voltage tower.

So this paper uses the field experiment and numerical simulation to study the vibration velocity and the main frequency of the high-voltage tower based on the record data in the process of blasting construction. In addition, some key positions in the high-voltage tower require monitoring and protecting. The blasting excavation safety zone where blasting excavation needs to be carefully done is proposed, which can provide references for other similar projects.

2. Brief Description of the Project

The Chashan tunnel is a short shallow-buried tunnel with six lanes in both directions. It is located on the Leguang expressway in Guangdong Province, China, as seen in Figure 1. The tunnel passes through the shallow karst hills and river deposits where the stratum is predominantly limestone with thin-bedded shale. The corresponding geotechnical parameters of local site conditions are shown in Table 1. Furthermore, the left tunnel and right tunnel have a similar feature, in which the width of two tunnels is all approximately 18 m, and the height is approximately 12 m, as seen in Figure 2. And the distance between the two tunnels is about 11 m, the length of the left tunnel is 258 m, and the length of the right tunnel is 259 m. The high-voltage tower is located approximately 60 meters from the entrance of the left tunnel and less than 10 meters from the center line of the left tunnel. The vertical distance between the tunnel and the high-voltage tower is approximately 37 meters. The monitoring points are arranged on the high-voltage tower foundation and tower main frame. The high-voltage towers are made of steel that are as high as 30 m, and the horizontal spacing between two foundations at the same side is 8 m, which is with a cup shape, and a spatial tower structure is composed of ideal hinge bars. This tower is made of Q_{235} or Q_{345} steel angles, where Q_{235} is the carbon steel and Q_{345} is the alloy steel (the letter Q represents yield strength) [38, 39]. Table 2 shows the parameters of the tower material.

3. Blasting Construction and Field Test

3.1. Blasting Pattern. According to the geographic environment and technology conditions of the Chashan tunnel, a three-benching blasting excavation method on the working face was proposed to control the quantity of blasting explosives and reduce the impact of blasting on the disturbance of the high-voltage towers. The distance between upper bench and second bench was controlled within 5 m. The blasting pattern is shown in Table 3. The periphery holes and auxiliary holes are in the same vertical plane. The layout of blasting holes is shown in Figure 3. Due to the large excavation area of the upper bench, the vibration intensity induced by the blasting is greater, so the research mainly focuses on the excavation blasting induced by vibration of the upper bench.

3.2. Blasting Monitoring. Blasting vibration monitoring is mainly to study the influence of shallow tunnel blasting excavation on the high-voltage tower. TOP-BOX blasting vibration recorder and digital blasting vibration wave analysis software are used in this blasting monitoring, and its sampling frequency is in the range of 50–200 Hz that fully record the potential frequency ranges of the tower vibration induced by the blasting construction [40]. In the process of blasting excavation, the sensor installed at the monitoring point vibrates with the vibration of the monitoring point. The principle of the instrument is to convert the relative motion kinetic energy between the magnetic coil systems into an electromotive force signal, the electromotive force signal is input into the computer through various hardware devices, and the waveform analysis and data processing software are used for data acquisition and storage. The schematic illustration of the vibration monitoring system is shown in Figure 4.

To study the influence of blasting construction on the high-voltage tower, before the blasting excavation, the measuring point is installed on the surface of the tower foundation and main frame of the tower to record the peak velocity and frequency of the high-voltage tower in the

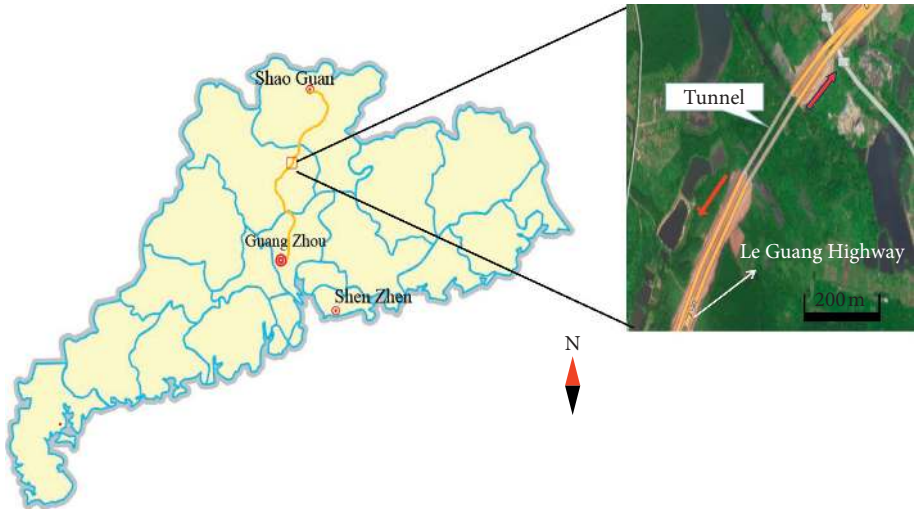

Figure 1: Location of the tunnel.

Table 1: Parameters of local site conditions.

Type	E (GPa)	γ (KN/m^3)	λ	V_s (km/s)
Sand soil	0.2	18.2	0.31	0.7
Bedded shale	11.1	22.1	0.29	3.8
Limestone	28.5	20.9	0.29	5.2

E: elastic modulus; γ: unit weight; λ: Poisson's ratio; V_s: compressive wave velocity.

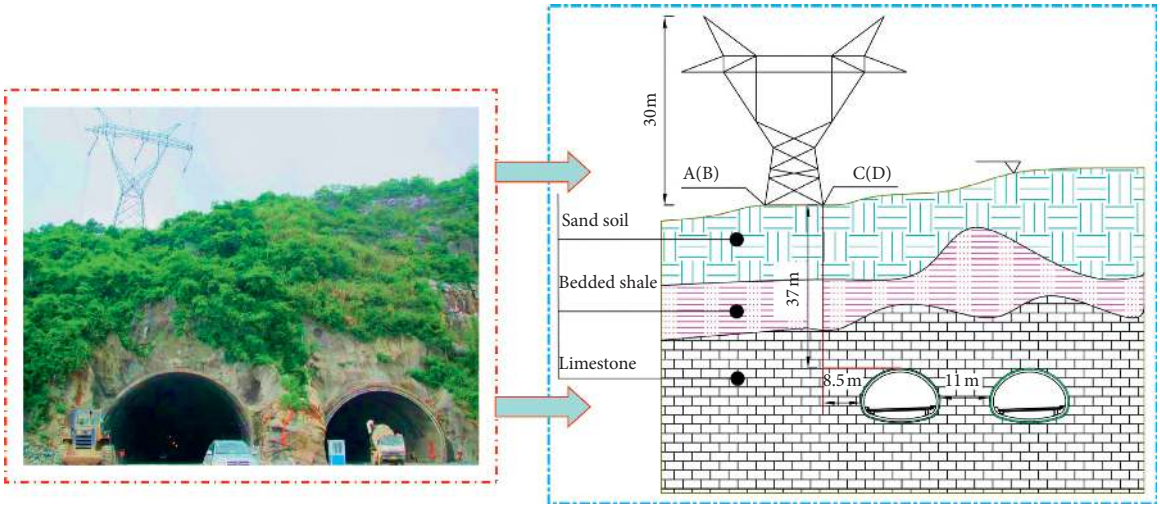

Figure 2: Cross section of the tunnel and geological information of entrance portion.

Table 2: Parameters of the tower material.

Steel material	σ_y (MPa)	E (GPa)	λ
Q_{235}	235	201	0.3
Q_{345}	345	206	0.25

σ_y: yield strength; E: elastic modulus; λ: Poisson's ratio.

process of blasting construction. As shown in Figure 5, the four measuring points A, B, C, and D are, respectively, distributed on the foundation of the high-voltage tower to record the velocity amplitude, time history curve, and vibration energy spectrum in the process of tunnel blasting. And three measuring points are implemented along with the vertical direction of the tower frame to analyze comprehensively the vibration characteristics of the high-voltage tower. The height of the measuring points is 10 m, 20 m, and 28 m distance from the surface, respectively. However, due to the undulating terrain, the propagation law of blasting vibration waves has its particularity that, during the blasting construction, the vibration response of the ground surface directly above the excavation face may not be the most serious. The monitoring range of the tower takes 60 m along the tunnel for the origin. Figure 6 shows the sectional view of blasting excavation, the detonation center is O, the tower

Table 3: Blasting pattern.

Excavation site	Blasting parameters	Number of holes	Hole of depth (m)	Charge weight per hole (kg)	Delay	Explosive weight per delay (kg)
Upper bench	Cut holes	6	1.2	0.6	1	3.6
	Auxiliary holes	29	1.0	0.8	3, 5, 7, 9	23.2
	Peripheral holes	31	1.0	0.29	11	8.99
Second bench	Auxiliary holes	40	1.0	0.57	1, 3, 5, 7, 9	22.8
	Peripheral holes	16	1.0	0.29	16	4.64
Lower bench	Auxiliary holes	30	1.0	0.57	1, 3, 5, 7	17.1
	Bottom plate holes	20	1.0	0.57	9	11.4

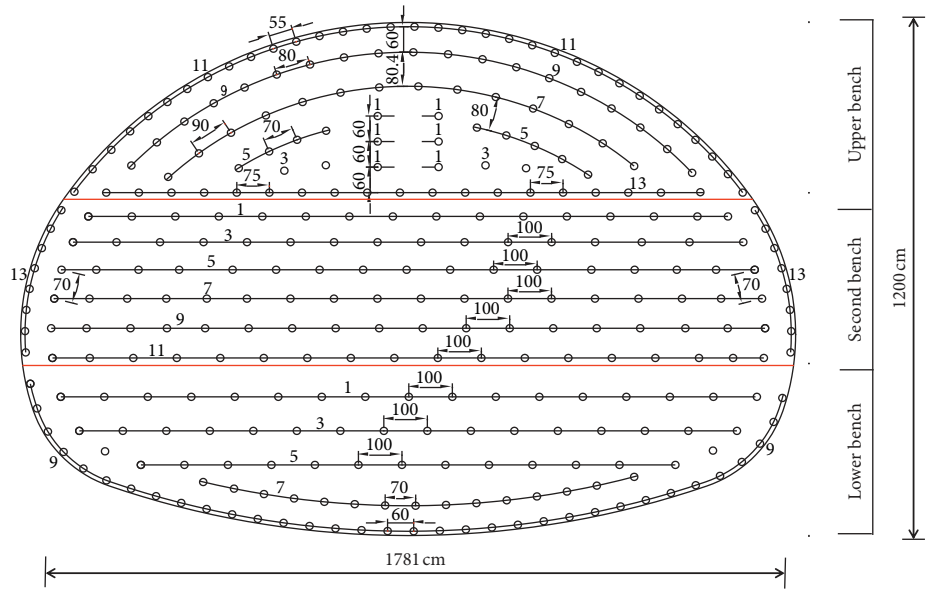

Figure 3: Layout of blasting holes.

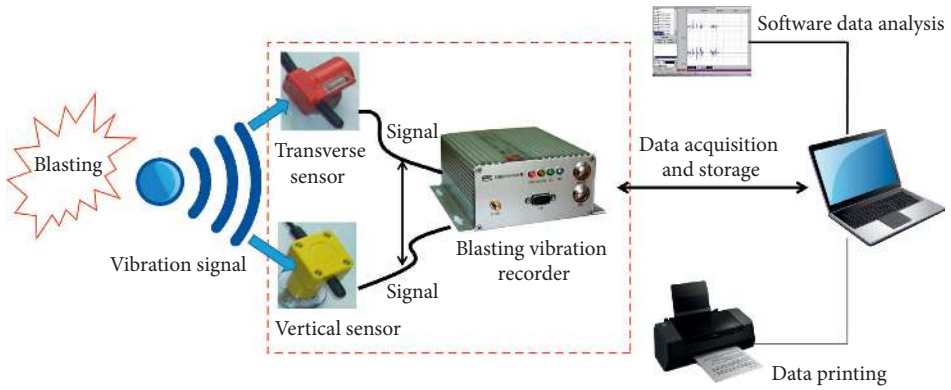

Figure 4: Vibration monitoring system.

foundation is T, the longitudinal distance between the detonation center and tower foundation is L, the vertical distance between the detonation center and the tower foundation is H, the distance between the detonation center and the tower foundation is R', and R is the projection along the longitudinal plane in distance between the tower foundation and detonation center.

3.3. Test Results. Since the left tunnel is excavated first, this paper mainly focuses on the influence of blasting excavation of the left tunnel on the tower. However, to limit the amount of data included in this paper, the following results only focus on the velocity-time history curve of point D when L is 0 m. The results are shown in Figure 7, and the time interval between detonators is 0.1 s during the blasting. And, thus the

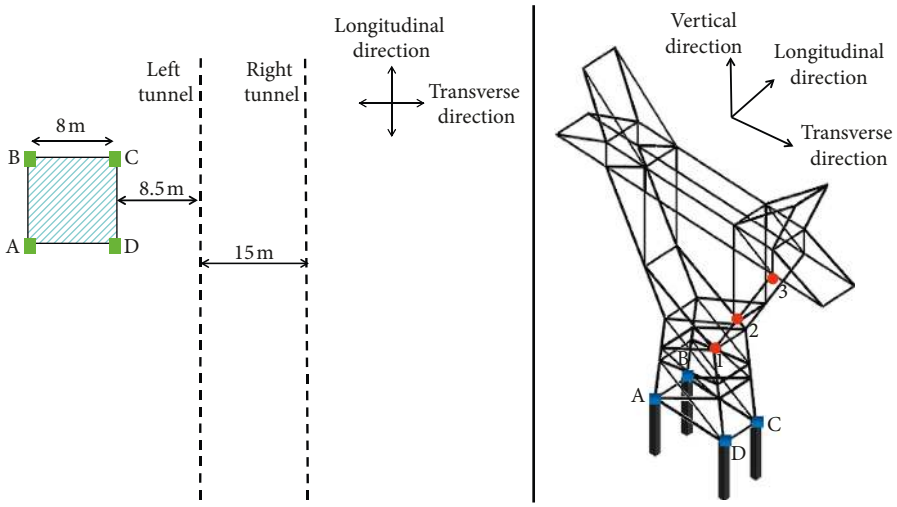

Figure 5: Measuring point arrangement.

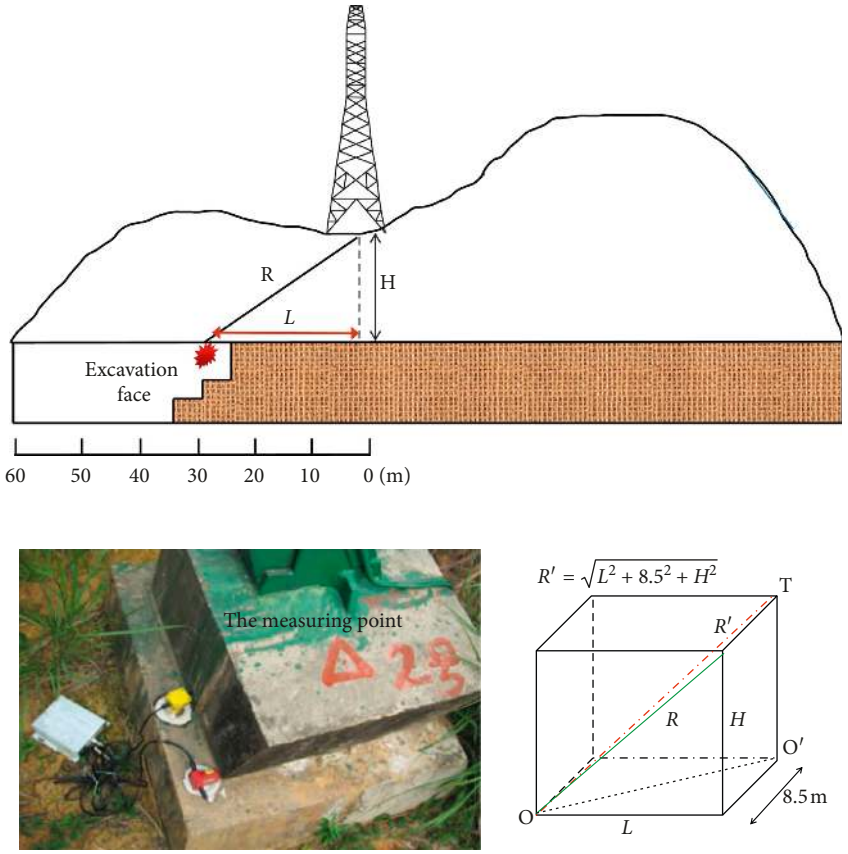

Figure 6: Sectional view of blasting excavation.

reflection of explosion waves occurred at interfaces of different media leads to a plurality of peak troughs appearing in the vertical velocity, where maximum velocity was 1.75 cm/s at $t = 0.25$ s, and the blasting vibration time lasted approximately 1.0 s. Moreover, the peak velocity in the vertical direction was larger than the transverse direction.

Table 4 records the vertical, transverse, and longitudinal velocity and main frequency of point D, when L was 60 m, 50 m, 40 m, 30 m, 20 m, 10 m, and 0 m in the process of blasting excavation. The effect of blasting vibration on the tower was summarized as follows: as the distance between the detonation center and tower foundation approaches, the velocity in three directions of point D was greater. When the distance between the tower foundation was zero, the velocity in three directions of point D reaches the maximum. And, in the field experiment, vertical vibration velocity was maximal

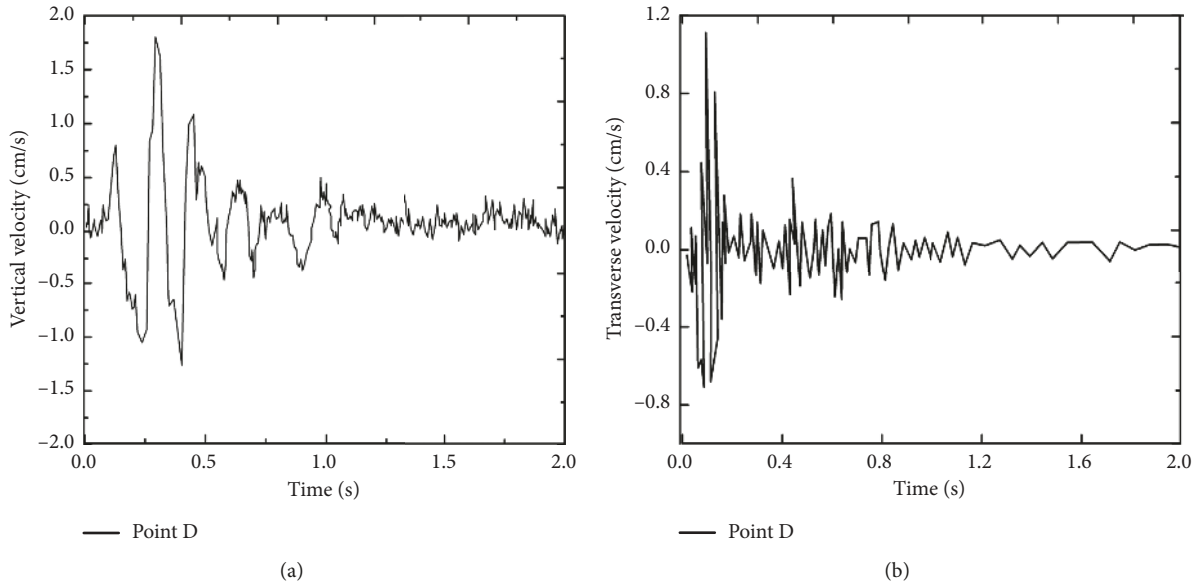

Figure 7: Velocity time histories of measuring point D when blasting distance is 0 m: (a) vertical direction; (b) transverse direction.

Table 4: Maximum velocity and frequency of point D.

Test number	L	R'	Velocity (cm/s)			Frequency (Hz)		
			Longitudinal	Transverse	Vertical	Longitudinal	Transverse	Vertical
1	60	71.00	0.0155	0.1026	0.0925	12.23	14.02	18.13
2	50	62.77	0.0239	0.2016	0.2579	9.26	12.23	16.26
3	40	55.14	0.0356	0.4539	0.4835	12.65	10.10	24.12
4	30	48.38	0.0688	0.6348	0.7148	23.56	23.36	32.39
5	20	42.90	0.0672	0.7541	0.8469	26.79	32.31	56.26
6	10	39.25	0.1078	0.8247	1.4269	57.24	50.31	70.23
7	0	37.96	0.1536	1.4406	2.3580	79.53	87.61	90.24

L: longitudinal blasting distance; R': the distance between detonation center and tower foundation.

among the three directions, which was perpendicular to the foundation of the exiting tower. Based on the safety criterion of blasting vibration velocity for different structures according to the Chinese code for blasting safety standards (1999), it can be found that the allowable vibration velocity was no more than 2.5 cm/s. When the detonation distance is 0 m, the maximum vibration velocity was 2.358 cm/s in measuring point D, which is close to the safety control standard of 2.5 cm/s. Therefore, for eliminating potential safety hazards as early as possible and preventing the collapse of the tower, the monitoring of the tower foundation should be strengthened and the blasting charge should be reduced during the blasting construction.

Figure 8 shows the distribution of the maximum vertical velocity of the four measuring points in the tower foundation. Although the maximum velocity does not occur simultaneously at all nodes, they are presented and compared to examine the relative effect of the tower foundation location. It can be seen that the peak velocity of the four measuring points occurring at point D (2.5 cm/s), and the rest at point A-B-C are 1.25 cm/s, 2.0 cm/s, and 1.85 cm/s, respectively. Compared with the maximum velocity in other directions, the maximum velocity of the four measuring points fluctuates greatly in the vertical direction. Furthermore, with regard to the distance between the blasting center and tower foundation, the fluctuation range of the maximum velocity of the four measuring points is smaller. Figure 9 shows that the relationship between the detonation distance and the vertical velocity of the four measuring points is as follows: the closer the distance between longitudinal detonation centers is, the faster the attenuation of vibration velocity is, and the farther the distance between longitudinal detonation centers is, the slower the attenuation of vibration velocity is, and the overall nonlinear attenuation is presented. The following equation shows the attenuation relationship between the detonation distance and the vertical velocity in measuring point D:

$$y = 0.096 + 2.235 \times 0.952^{x}, \quad (1)$$

where x is the blasting distance and y is the vertical velocity.

It can be clearly seen from the vertical vibration velocity diagram that the vibration velocity of the tower foundation in point D is the largest under the same blasting distance, and the attenuation law of vibration velocity in tower foundation measuring points C and A have little difference.

However, due to the undulating terrain, the propagation law of blasting vibration waves has its particularity that the vibration response of the ground surface directly above

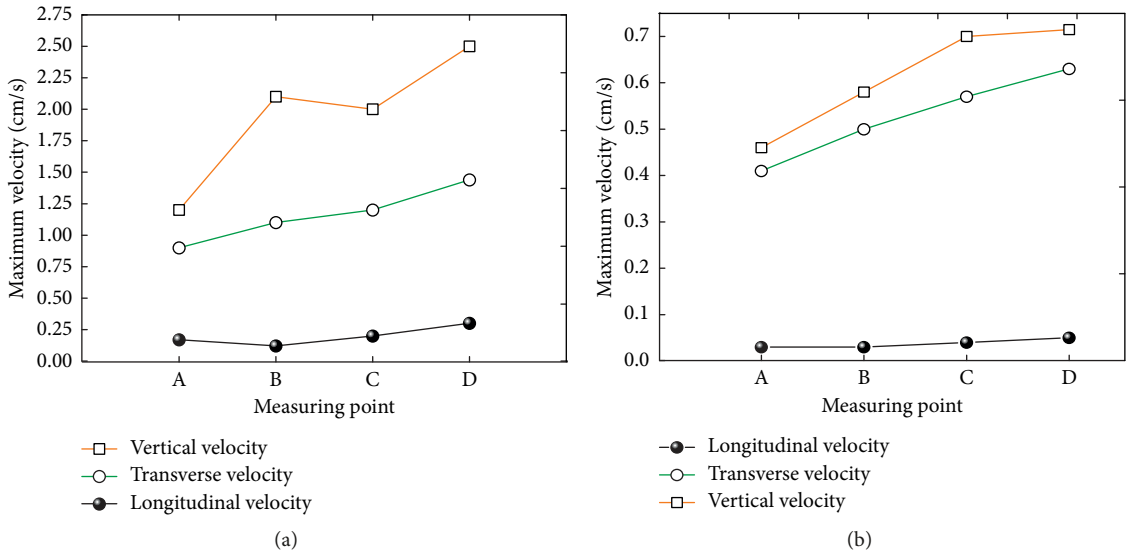

Figure 8: Distribution of maximum velocity. Blasting distance: (a) 0 m; (b) 30 m.

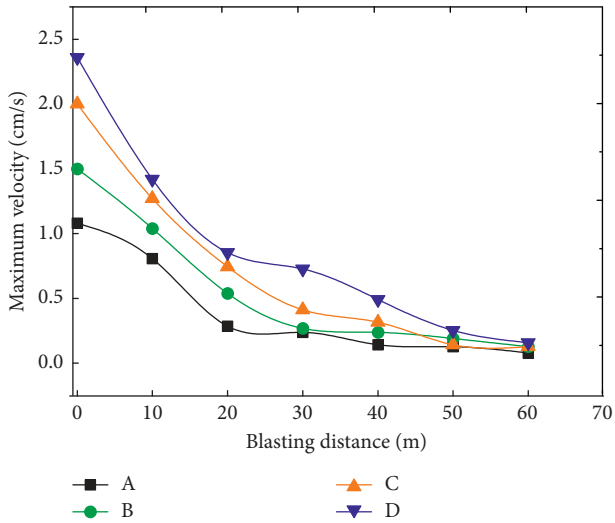

Figure 9: Variations of vertical velocity.

the excavation face may not be the most serious. Therefore, for further research based on the damage mechanisms induced by blasting vibration, scholars found that blasting vibration damage of tunnels is closely related with not only peak velocity but also its dominant frequency [41, 42]. More and more engineering practices show that it is not comprehensive to adopt a single peak velocity as safety criterion [43–45]. So it is reasonable to consider the combination of blasting vibration frequency and vibration velocity to evaluate the safety of surrounding buildings of the tunnel. The vibration frequency of the measuring point is mainly affected by the distance between detonation centers, the scale of blasting, and the characteristics of the propagation medium. Although the frequency distribution of the blasting vibration wave is relatively scattered, the vibration wave that causes the engineering problem is mainly caused by the frequency of the blasting vibration wave concentrate near the main frequency of buildings, which may cause a local or overall resonance effect of the building, causing damage to the surrounding buildings. Figures 10 and 11 show the energy spectrum of three directions of the vibration signal at monitoring point D in TN7 and TN3 at the field experiment (the TN letters represent the test number). Based on the analysis of the monitoring data, as shown in Table 4, the vertical vibration frequency of point D is generally higher than in the transverse direction. Figure 10 shows that vertical blasting vibration energy concentrates on 20~30 Hz in the TN3, vertical main frequency at 24.12 Hz, transverse blasting vibration energy concentrates on 3~10.5 Hz in the TN3, and transverse main frequency at 10.1 Hz. Meanwhile, the vertical blasting vibration energy is concentrated on 80~100 Hz in the TN7 and vertical main frequency at 89 Hz. The transverse blasting vibration energy is concentrated on the 50~90 Hz and transverse main frequency at 80 Hz. Apparently, the blasting vibration energy of the TN3 position is much smaller than the TN7. This is because with the increase of propagation distance, the high-frequency component of the blasting vibration wave attenuates faster than the low-frequency component because of the large damp in rock and soil and the selective absorption of the blasting vibration wave frequency by rock and soil medium [46]. Therefore, the distance between detonation centers at the TN3 field experiment is 54.49 m, the low frequency of the blasting vibration wave is concentrated, the distance between detonation centers at the TN7 field experiment is 37.00 m, and the high frequency of the blasting vibration wave is concentrated.

From the existing data [47, 48], it can be concluded that the natural frequency of tower ranges from 2.43 Hz to 10.68 Hz, which belongs to the lower frequency. When the main frequency of the blasting vibration wave is in the range of 2–11 Hz, even if the vibration velocity is relatively smaller, it may cause damage to the tower. Combining the existing monitoring data of Table 4 and Figures 10 and 11, it can be obtained that, when the L is 0 m, the maximum velocity of

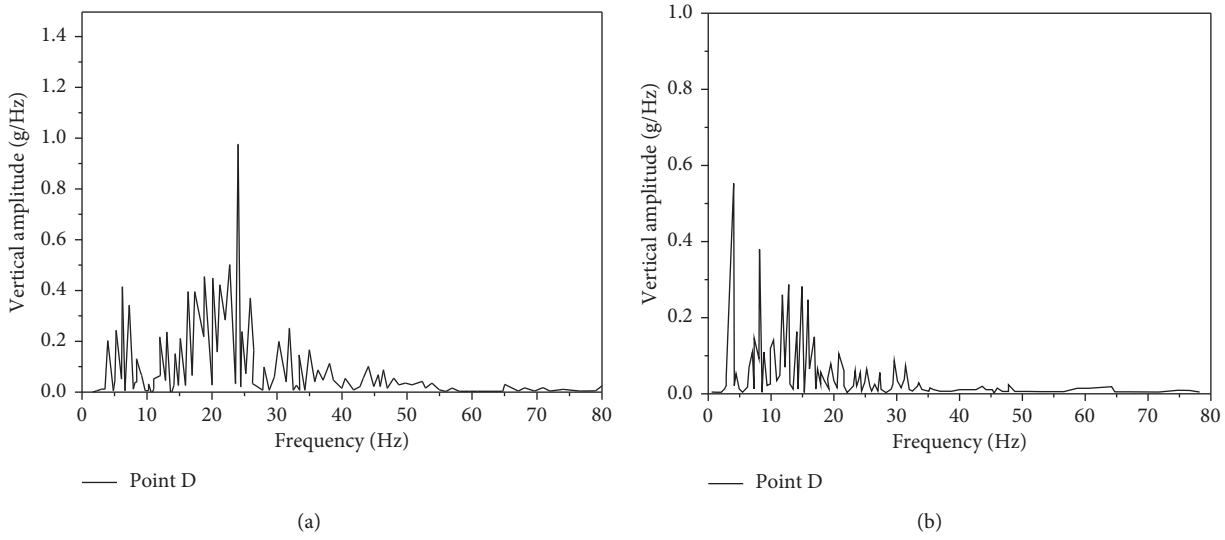

Figure 10: Energy spectrum of monitoring point D in TN3: (a) vertical; (b) transverse.

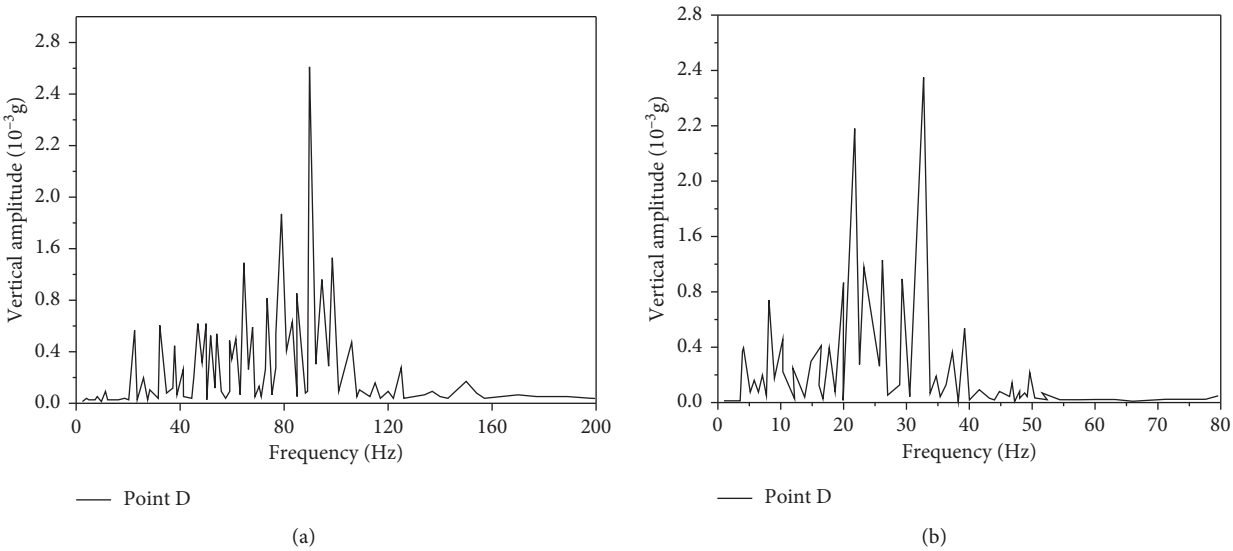

Figure 11: Energy spectrum of monitoring point D in TN7: (a) vertical; (b) transverse.

the measuring point is 2.35 cm/s, which is approximately to exceed the critical value of safe velocity of 2.5 cm/s, and the main frequency is 90.24 Hz; on the other hand, when the L is 30 m, the maximum vibration velocity is 0.48 cm/s. At this time, the main frequency of the blasting vibration is 10.1 Hz, which is already within the natural frequency of the tower range of 2~11 Hz, which may result in tower to damage.

4. Numerical Simulation and Analysis

4.1. Model. To compare numerical simulation results with the field measurement results, as well as to more fully understand the vibration characteristic of the tower main frame under the blasting, a three-dimensional finite element model was established by Midas-GTS finite element software, which was generally used to conduct the geotechnical analysis. Based on St. Venant principle [49, 50], it is appropriate to take three times of the size of tunnel face for left, right, and bottom parts of the model to reduce the influence of boundary effects. So, the model size is 150 m × 120 m × 90 m, as shown in Figure 12. The tunnel and surrounding rock adopts three-dimensional solid elements to simplify the high-voltage towers into beam structures, and this tower's auxiliary material is Q_{235} steel with an elastic modulus of 201 MPa. The tower foundation adopts pile element, and surrounding rock adopts ideal Mohr–Coulomb's failure criterion in the calculation. Based on the actual engineering geology situation, it is assumed that the rock mass and the surrounding rock are continuous media, and a IV-grade surrounding rock is adopted in the numerical simulation. Surrounding rock classification according to rock classification BQ (basic quality) (Ministry of Water Resources of the People's Republic of China, 1995) and "Code for Design of Railway Tunnel," a viscous

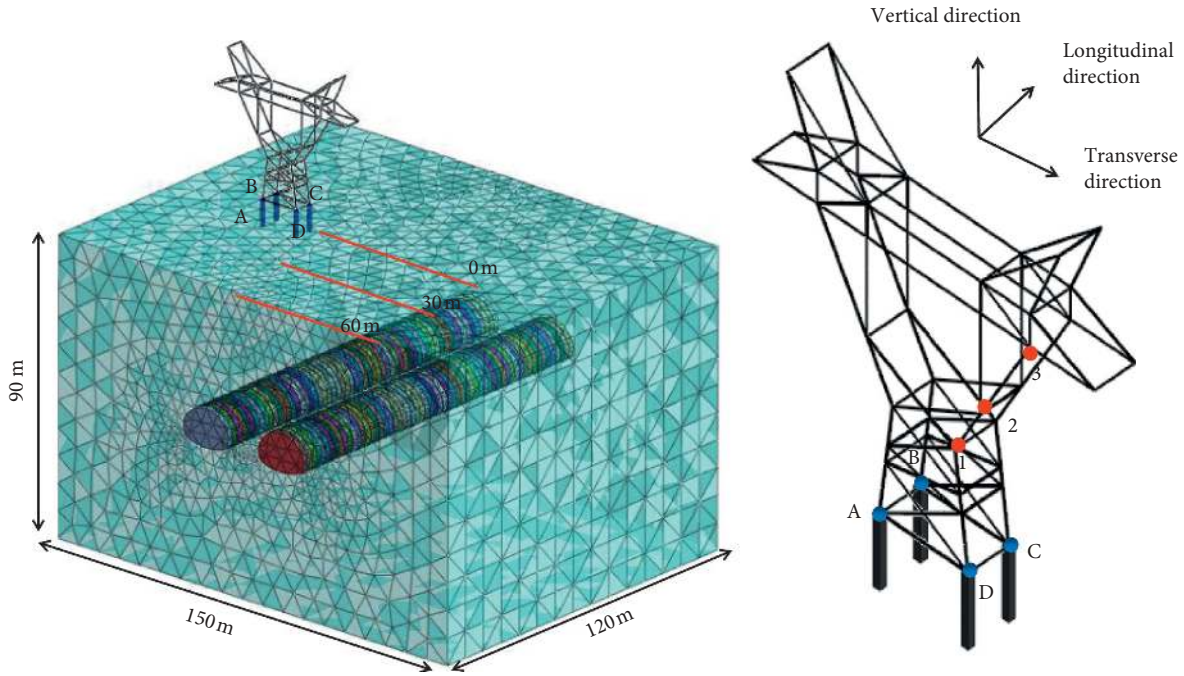

Figure 12: Finite element model of the tunnel and tower.

boundary is used on the bottom and sides of the model, which is equivalent to set a separate damper at the boundary [51–54]. In the finite element software, first enter the unit area damping constants c_s and c_p and then the software will automatically calculate the cross-sectional area of each unit and apply the point spring to the unit node to form the model boundary.

Here, this model load only considers the self-weight stress and the blasting load. The effect of the transmission cables connected to the high-voltage tower is considered in the form of an equivalent static load. Therefore, the tower-cable interaction is not considered in the vibration analysis [55]. To accurately understand the vibration velocity and vibration frequency of the high-voltage tower during tunnel blasting excavation, the effects of tunnel blasting excavation on the tower, under the seven conditions that detonation center distance is 60 m, 50 m, 40 m, 30 m, 20 m, 10 m, and 0 m, respectively, are discussed. In addition, in the blasting dynamic analysis, the static parameters of surrounding rock and concrete materials are improved under the condition of high strain rate or blasting impact due to the strain rate effect. So this paper adopts the dynamic parameter, where the empirical formula of dynamic parameters is as follows:

$$E_d = 8.577E_s^{0.5882}, \tag{2}$$

where E_s is the static modulus of elasticity and E_d is the dynamic modulus of elasticity [56].

Dai [57] through the research shows that, in the range of loading frequency of engineering blasting, the dynamic Poisson's ratio is about 0.8 times the static Poisson's ratio. The model parameters are revised according to the research results of the above scholars. The model parameters after revision are illustrated in Table 5.

Table 5: Model parameters.

Material type	E (GPa)	γ (kN/m^3)	μ	C (MPa)	θ (°)
Surrounding rock	18.3	21.6	0.24	0.63	36
Initial lining	35	23	0.16	0.63	36
Anchor	210	78.5	0.3	—	—
Tower	201	78	0.2	—	—
Tower foundation	30	23	0.25	—	—

E: elastic modulus; γ: bulk density; μ: Poisson's ratio; C: cohesion; θ: internal friction angle.

4.2. Blasting Load. For simplify the model of the blasting hole, it is assumed that all the blasting holes are concentrated in one position. As shown in Figure 13, the load pressure acts on the blasting tunnel wall at the same time, and the acting direction is perpendicular to the normal of the surrounding rock.

When calculating the blasting load, the detonating pressure is loaded in the vertical direction of the borehole wall. A large part of the blast energy is dissipated during the fracturing of the rocks the charged borehole, as shown in Figure 14 [58]. The load formula used is the formula mentioned in National Highway Institute of the United States [59]. The detonating pressure per kg is as follows:

$$P_{det} = \frac{4.18 \times 10^{-7} \times S_{ge} \times v_e^2}{1 + 0.8S_{ge}},$$
$$P_B = P_{det} \times \left(\frac{d_c}{d_h}\right)^3, \tag{3}$$

where P_{det} is the detonating pressure in the hole, P_B is the decoupled detonation pressure, S_{ge} is the explosive density (g/cm^3), d_c is the charge diameter (m), d_h is the borehole diameter (m), and v_e is the detonation velocity (m/s).

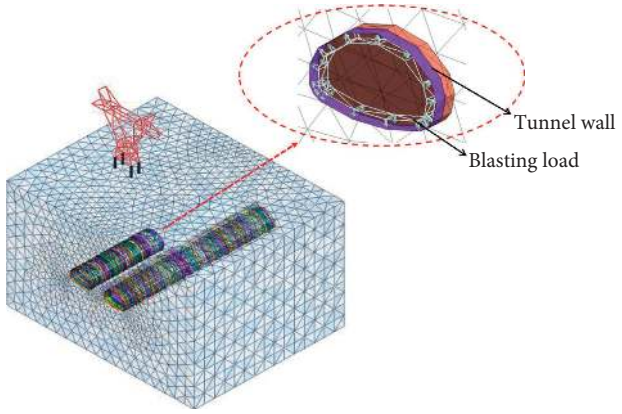

Figure 13: Schematic diagram of blasting load.

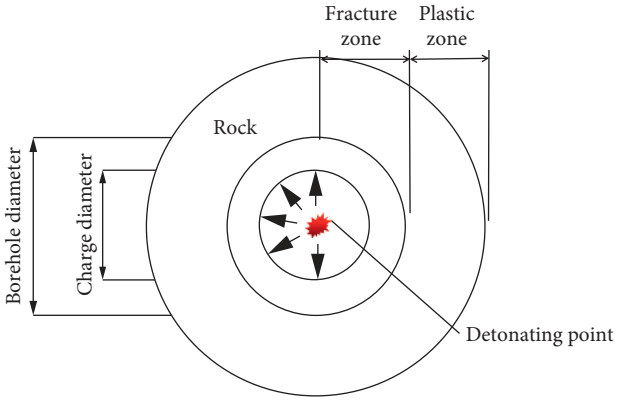

Figure 14: Pressure mechanism.

The detonating pressure may be characterized as a pulse with an exponential shape time history that attenuates rapidly in amplitude and broadens as it propagates outward from the detonation center. Thus, it is also necessary to establish the variation and decay of the incident pressure with time because the effects on the tower depend not only on the peak pressure but also on the pressure-time history of the blast loading. Therefore, the formula of time history detonation pressure is adopted:

$$P_{\mathrm{D}}(t) = 4P_{\mathrm{B}}\left(\exp\left(\frac{-B\cdot t}{\sqrt{2}}\right) - \exp\left(-\sqrt{2}\,B\cdot t\right)\right), \quad (4)$$

where B is the empirical load coefficient (=16,338), P_{D} is the detonation pressure per 1 kg charge, and t is the time.

Time histories of blasting load are shown in Figure 15.

4.3. Simulation Result and Comparison

4.3.1. Analysis of Tower Foundation. To fully understand the dynamic response of the high tower during the blasting excavation and to better test the validity of the field test results, the velocity values of the measured point D under a different distance of the detonation center are obtained by using the finite element model [60–62]. The layout of model points is shown in Figure 5. Table 6 is a comparison between the numerical simulation results and the field test results,

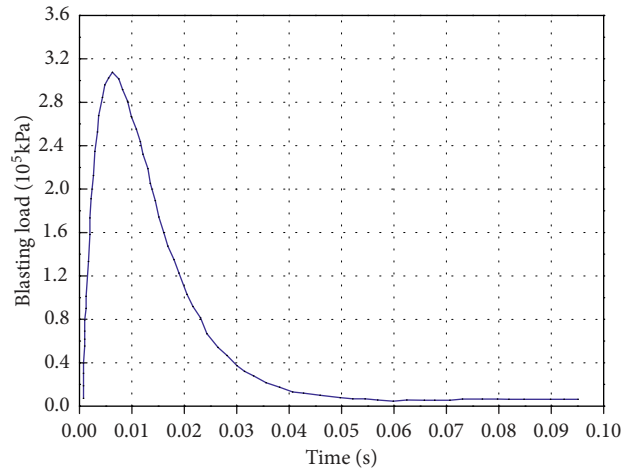

Figure 15: Blasting load time histories.

and it can be seen from the table that the velocity responses of the tower main frame obtained from the numerical simulation are in accordance with those from field monitoring data, even if the difference of response amplitude exists. A couple of comments are given to explain the difference: the parameters used in the numerical analysis of the tower structure subjected to the blasting loads may be divided into two major groups: surrounding rock parameters and blasting characteristics; the surrounding rock parameters are determinable or controllable where the blasting characteristics are most likely undetermined or uncontrollable.

Through numerical simulation, the comparison results of velocity history time between the field test and numerical analysis of point D are obtained. As shown in Figure 16, the vertical velocity and transverse velocity have similar shape and characteristics with the field test. After blasting, the response amplitude of vibration velocity increases obviously; the waveform fluctuates greatly, as time approaches infinity and the velocity responses all diminish to zero. Furthermore, vertical velocity of the measuring point is obviously greater than transverse velocity. Table 6 shows that the maximum transverse and vertical velocities are 2.3 cm/s and 1.16 cm/s, respectively, in point D.

4.3.2. Vibration Velocity. In response to more comprehensively analyze the dynamic response of blasting vibration to the high tower above the tunnel and combined with the existing research conclusions, the vibration velocity response of the measuring points at different heights of the high tower is analyzed.

Figure 17 shows the peak velocity of particles in three directions when the L is 0 m. The peak vibration velocity increases with the height of the particle and reaches a maximum at the top of the tower. When the height of the particle is 30 m, the maximum velocity of the vertical vibration is 4.12 cm/s. Compared with the transverse velocity of 1.44 cm/s and the longitudinal velocity of 1.79 cm/s, the vertical vibration velocity has a great influence on the tower, and this should be taken seriously. The particle velocity at the

Table 6: Summary of the maximum velocity results in point D.

Test number	L	R'	Max v (field measurement) (cm/s)			Max v (numerical simulation) (cm/s)		
			Longitudinal	Transverse	Vertical	Longitudinal	Transverse	Vertical
1	60	71.00	0.0155	0.1026	0.0925	0.019	0.1121	0.08
2	50	62.77	0.0239	0.2016	0.2579	0.0211	0.2004	0.2451
3	40	55.14	0.0356	0.4539	0.4835	0.0284	0.4462	0.4729
4	30	48.38	0.0688	0.6348	0.7148	0.0594	0.5763	0.7012
5	20	42.90	0.0672	0.7541	0.8469	0.0631	0.7421	0.8416
6	10	39.25	0.1078	0.8247	1.4269	0.1024	0.8127	1.5243
7	0	37.96	0.1536	1.0406	2.3580	0.1496	1.0241	2.192

L: longitudinal blasting distance; R': distance between detonation center and tower foundation.

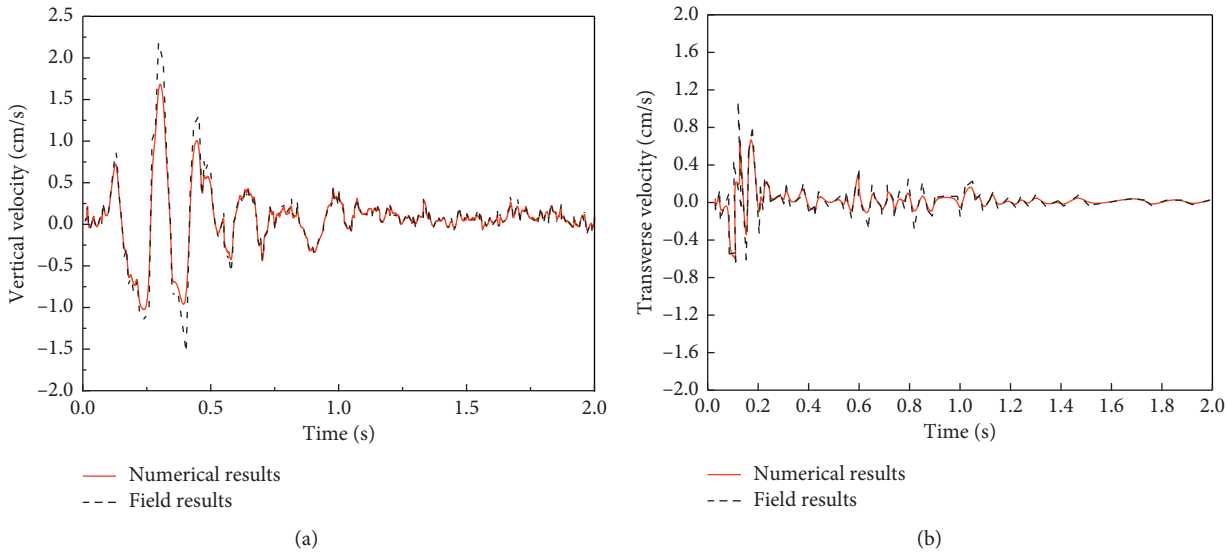

Figure 16: Time histories of velocity in point D when L is 0 m: (a) vertical velocity; (b) transverse velocity.

height of 0 m is the velocity of the measured point of the tower foundation. It can be seen that the peak velocity of the three directions of blasting is greater than the peak velocity of tower foundation during the process of blasting at any height of the particle in the tower. It shows that the vibration velocity of the tower has an amplification effect under the blasting vibration.

As shown in Figure 17, there are some difference between field test data and numerical data, but both fit well. The maximum difference is 0.5 cm/s which occurs at point 1 in the vertical direction. Due to the presence of jointed rock in actual projects, rock in numerical simulation is assumed the homogeneous body, so a small deviation of the results can be understood. In addition, the particle velocity generally shows an upward trend.

4.3.3. Tower Axial Force. Figure 18 shows the maximum axial force distribution of the tower member at different heights in the process of blasting construction. The maximum axial force decreases gradually with the increase in height of the measuring point. When the measuring point height is greater than 12 m, the maximum axial force decays slowly and gradually stabilizes. In general, at the same height of the tower, the axial force value increased with an decrease in distance between the detonation centers and tower. The maximum value of the axial force that occurs at the tower bottom is 14.8 kN when the distance between the detonation centers is 0 m.

4.3.4. Tower Foundation Displacement. The vibration velocity reaches the maximum value, when the longitudinal distance between the tower and the detonation center is 0 m, which easily causes strong disturbance to the tower, and the tower foundation is prone to uneven settlement leading to the inclination of the tower. Therefore, the displacement of tower foundation is analyzed when the tower and the detonation center is 0 m. Figure 19 shows the displacement-time history curve of the measuring point of the tower foundation: the positive value represents the uplift, and the negative value represents the settlement. After blasting, the displacement value of the measuring point increases obviously and reaches the maximum value when $t = 0.01$ s. As time approaches infinity, the displacement value attenuates notably and gradually stabilizes. The peak values of transverse and longitudinal displacement are −0.14 mm and 0.065 mm, respectively, which have little influence on the stability of the tower. The figure reveals that the maximum vertical displacement value is 0.28 mm located at point D,

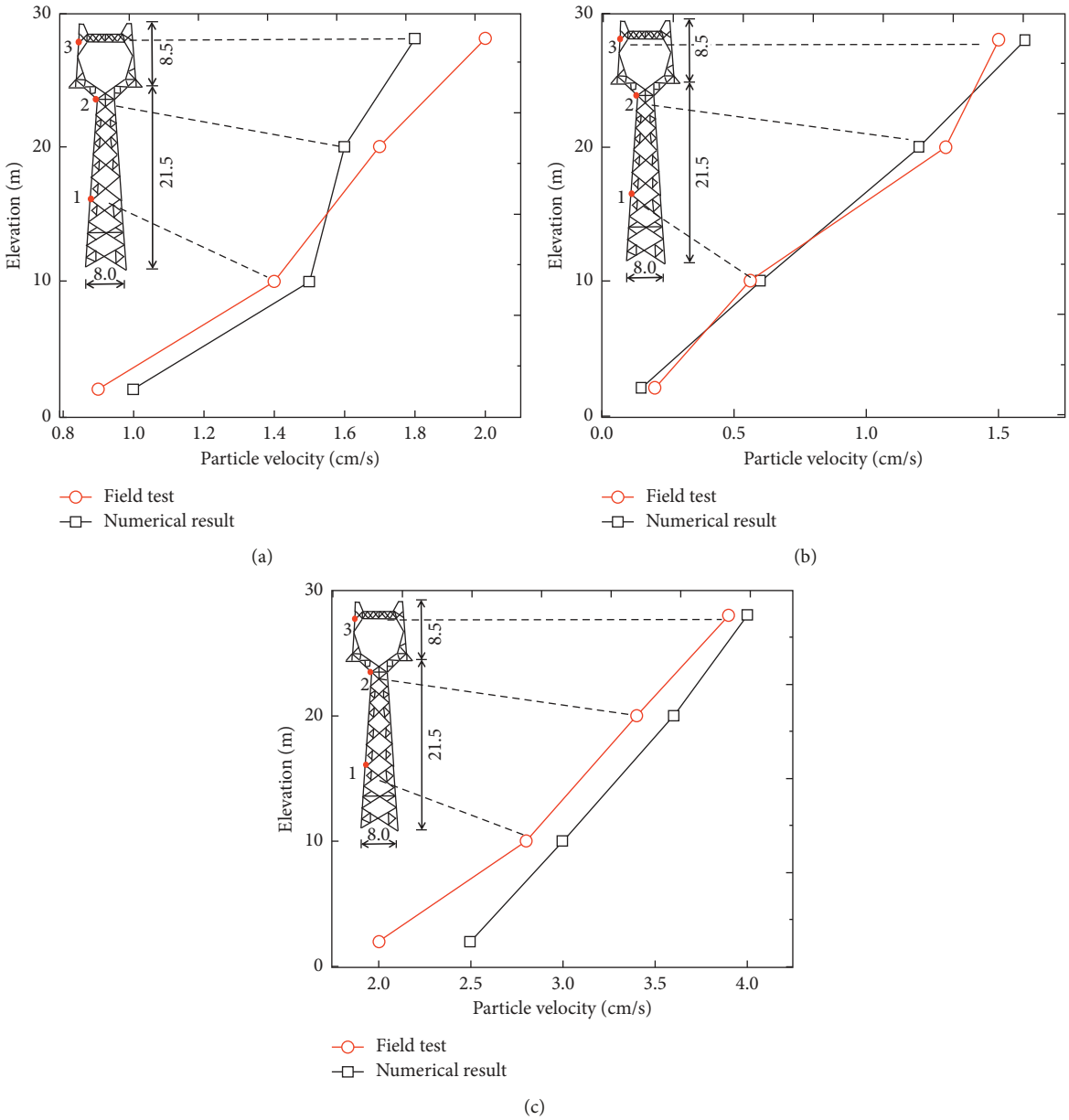

Figure 17: Measuring point velocity along the tower elevation when L is 0 m: (a) transverse direction; (b) longitudinal direction; (c) vertical direction.

and the minimum vertical displacement value is 0.16 mm located at point A. The settlement difference between the measuring points is only about 0.12 mm. According to the specification, the uneven settlement value of the tower foundation is within the safety range, which will not cause the tower to incline or collapse.

5. Discussion

Based on the monitoring data and numerical results of the tower subjected to blasting loads, the maximum vertical and transverse velocities of the tower foundation are 2.358 cm/s and 1.04 cm/s, respectively, when blasting distance is 0 m. The former value is quite close to the allowable upper limits of 2.5 cm/s based on the Chinese code for blasting safety standards (1999), and so the performance of the tower under the blasting construction is in a critical state of safety. Moreover, at this time, the main frequency of blasting is in the range of 80.2 Hz~90.24 Hz. It can be taken as an indication that the blasting construction scheme should be implemented carefully. When the distance between the detonation centers is 30 m, the maximum vibration velocity of the measuring points is 0.48 cm/s. At this time, the blasting vibration velocity is smaller than the limiting blasting velocity, and the transverse blasting main frequency is 10.01 Hz. Through a number of field model tests of the existing high-voltage tower structure, it can be concluded that the tower natural frequency is approximately in the range of 2.43–10.68 Hz, which belongs to the lower frequency. Therefore, when the main frequency of tower, under

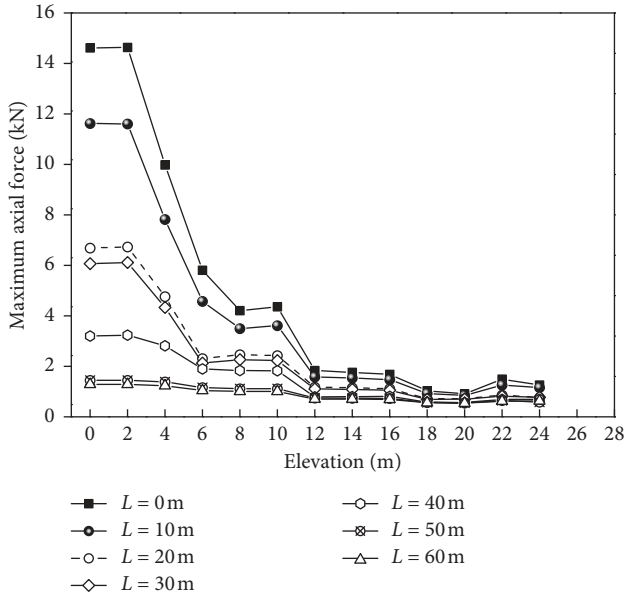

Figure 18: Maximum axial force.

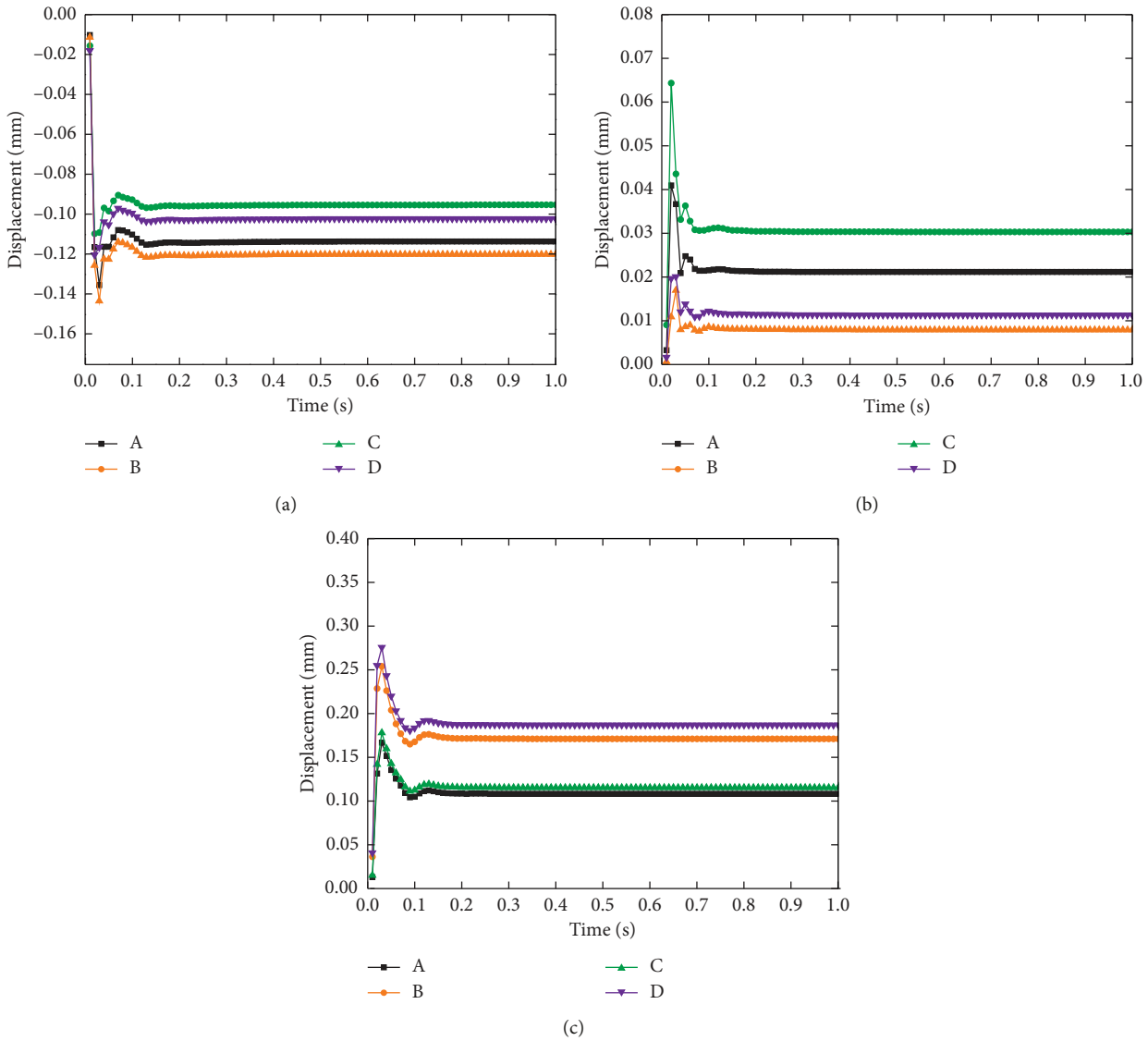

Figure 19: Displacement-time history curve: (a) transverse direction; (b) longitudinal direction; (c) vertical direction.

the process of blasting, is within its natural frequency range, even if the vibration velocity is small, it may cause the resonance damage of the tower. When the detonation center distance is 30 m, the difference between the main frequency and the natural frequency of the tower is small, which may cause the resonance damage of the tower.

Therefore, for reducing the impact of blasting excavation on the tower in the process of tunnel construction, it is necessary to adopt reasonable and reliable blasting parameters or construction schemes. The following recommendations are made.

(1) When the detonation distance is 30 m, the blasting vibration velocity is small, which has no effect on the high tower, but the smaller difference between the main vibration frequency and the natural frequency of the high tower is likely to cause the tower to be resonantly destroyed. Therefore, for reducing the effects of the blasting impact on the high tower, it is necessary to take measures to improve the overall stiffness and integrity of the tower or to set up vibration isolation ditches to reduce the output energy of the vibration induced by the blasting progress.

(2) When the detonation center distance is 0 m, the blasting vibration velocity has great influence on the existing tower, which is close to the safety critical value. It is necessary to change blasting parameters such as drilling depth and charge quantity or using electronic detonators to reduce blasting vibration.

(3) Some protect measures should be proposed when the longitudinal distance between detonation center and tower is around 30 m and 0 m.

6. Conclusion

A comprehensive field test has been carried out at high-voltage tower and tunnel to investigate and analyze the dynamic response of the tower during the tunnel excavation. The validation of field monitoring data is verified by comparison with numerical results. Based on the monitoring data and numerical results of the tower subjected to blasting loads, the following conclusions are drawn:

(1) When L is 0 m, the maximum vibration velocity was 2.358 cm/s in measuring point D, which is close to the safety control standard of 2.5 cm/s. The tower response decreases with the increase of distance from the detonation center, due to the diminution of the compressive waves in the surrounding rock. Moreover, the vertical velocity of the measuring points is obviously higher than that of other directions, which indicate that the blasting energy mainly propagates in the vertical direction.

(2) The vibration frequency of the measuring point D is measured. It illustrated that when the longitudinal blasting distance is 30 m, the main frequency of the blasting vibration is 10.1 Hz, which is close to the natural frequency of the tower, which is easy to cause resonance damage. The nearer the detonation centers is to the tower, the faster the attenuation of vibration velocity is, and the farther the distance is to detonation centers, the slower the attenuation of vibration velocity is. When the longitudinal distance between detonation centers and tower is 0 m, the vibration velocity is 2.38 cm/s, which is close to the safety critical value of 2.5 cm/s, which is easy to cause damage to the tower. So the blasting construction scheme should be implemented carefully when the longitudinal distance between detonation center and tower is approximately 30 m and 0 m.

(3) As for the main frequency of vibration, the main frequency of the vertical direction is generally higher than that of the transverse and longitudinal directions. The farther the detonation centers is from the tower, the lower the frequency is, and the nearer the detonation centers is to tower, the higher the frequency is.

(4) Irrespective of the height of the measuring point in the tower main frame, the three-direction peak velocity is greater than that of the measuring point of tower foundation. As the height of the measuring point in the tower main frame increases, the vibration velocity also increases and reaches the maximum at the top of the tower. Furthermore, the maximum axial force decreases gradually with the increase in height of the measuring point. When the tower measuring point height is greater than 12 m, the maximum axial force decays slowly and gradually stabilizes.

Data Availability

The data used to support the findings of this study are available from the corresponding author upon request.

Conflicts of Interest

The authors declare that there are no conflicts of interest regarding the publication of this paper.

Acknowledgments

This work was financially supported by the National Key R&D program of China (no. 2018YFC0808706) and the Project on Social Development of Shaanxi Provincial Science and Technology Department (nos. 2018SF-382 and 2018SF-378).

References

[1] H. Yu, C. Cai, A. Bobet, X. Zhao, and Y. Yuan, "Analytical solution for longitudinal bending stiffness of shield tunnels," *Tunnelling and Underground Space Technology*, vol. 83, pp. 27–34, 2019.

[2] H. Yu, Z. Wang, Y. Yuan, and W. Li, "Numerical analysis of internal blast effects on underground tunnel in soils," *Structure and Infrastructure Engineering*, vol. 12, no. 9, pp. 1090–1105, 2016.

[3] Y. Y. Li, W. S. Lin, and Y. W. Zhang, "Vibration characteristics and damage repair of the Railway tunnel base," *Advances in Civil Engineering*, vol. 2019, Article ID 1097203, 16 pages, 2019.

[4] Z. Zhou, Y. Dong, P. Jiang et al., "Calculation of pile side friction by multiparameter statistical analysis," *Advances in Civil Engineering*, vol. 2019, Article ID 2638520, 12 pages, 2019.

[5] Y. Fang, Z. Chen, L. Tao, J. Cui, and Q. Yan, "Model tests on longitudinal surface settlement caused by shield tunnelling in sandy soil," *Sustainable Cities and Society*, vol. 47, article 101504, 2019.

[6] R. Qiao, Z. Shao, W. Wei, and Y. Zhang, "Theoretical investigation into the thermo-mechanical behaviours of tunnel lining during RABT fire development," *Arabian Journal for Science and Engineering*, vol. 44, no. 5, pp. 4807–4818, 2019.

[7] Z.-F. Wang, S.-L. Shen, and G. Modoni, "Enhancing discharge of spoil to mitigate disturbance induced by horizontal jet grouting in clayey soil: theoretical model and application," *Computers and Geotechnics*, vol. 111, pp. 222–228, 2019.

[8] N. Jiang and C. Zhou, "Blasting vibration safety criterion for a tunnel liner structure," *Tunnelling and Underground Space Technology*, vol. 32, pp. 52–57, 2012.

[9] L. Ahmed and A. Ansell, "Structural dynamic and stress wave models for the analysis of shotcrete on rock exposed to blasting," *Engineering Structure*, vol. 35, pp. 11–17, 2011.

[10] X. L. Luo, X. Meng, W. J. Gan et al., "Traffic data imputation algorithm based on improved low rank matrix decomposition," *Journal of Sensors*, vol. 2019, Article ID 7092713, 10 pages, 2019.

[11] H. K. Verma, N. K. Samadhiya, M. Singh, R. K. Goel, and P. K. Singh, "Blast induced rock mass damage around tunnels," *Tunnelling and Underground Space Technology*, vol. 71, pp. 149–158, 2018.

[12] N. Innaurato, R. Mancini, and M. Cardu, "On the influence of rock mass quality on the quality of blasting work in tunnel driving," *Tunnelling and Underground Space Technology*, vol. 13, no. 1, pp. 81–89, 1998.

[13] K. Dey and V. M. S. R. Murthy, "Predicting overbreak from blast vibration monitoring in a lake tap tunnel–a success story," *Fragblast*, vol. 7, no. 3, pp. 149–166, 2003.

[14] Z. J. Zhou, J. T. Lei, S. B. Shi, and T. Liu, "Seismic response of aeolian sand high embankment slopes in shaking table tests," *Applied Sciences*, vol. 9, no. 8, p. 1677, 2019.

[15] X. L. Wang, J. X. Lai, R. Garnes, and Y. Luo, "On the support system for tunnelling in squeezing ground of qingling-daba mountainous area: case study from soft rock tunnels," *Advances in Civil Engineering*, vol. 2019, Article ID. 8682535, p. 12, 2019.

[16] Z.-F. Wang, W.-C. Cheng, and Y.-Q. Wang, "Investigation into geohazards during urbanization process of Xi'an, China," *Natural Hazards*, vol. 92, no. 3, pp. 1937–1953, 2018.

[17] H.-N. Li, F.-L. Bai, L. Tian, and H. Hao, "Response of a transmission tower-line system at a canyon site to spatially varying ground motions," *Journal of Zhejiang University-Science A*, vol. 12, no. 2, pp. 103–120, 2011.

[18] F. G. A. Al-bermani and S. Kitipornchai, "Nonlinear analysis of transmission towers," *Engineering Structures*, vol. 14, no. 3, pp. 139–151, 1992.

[19] H.-D. Zheng, J. Fan, and X.-H. Long, "Analysis of the seismic collapse of a high-rise power transmission tower structure," *Journal of Constructional Steel Research*, vol. 134, pp. 180–193, 2017.

[20] A. Ghobarah, T. S. Aziz, and M. El-Attar, "Response of transmission lines to multiple support excitation," *Engineering Structures*, vol. 18, no. 12, pp. 936–946, 1996.

[21] P. Zhang, G. B. Song, H. N. Li, and Y. X. Lin, "Seismic control of power transmission tower using pounding TMD," *Journal of Engineering Mechanics*, vol. 139, no. 10, pp. 1395–1406, 2013.

[22] J. Wang, Q. Huo, Z. Song et al., "Study on adaptability of primary support arch cover method for large-span embedded tunnels in the upper-soft lower-hard stratum," *Advances in Mechanical Engineering*, vol. 11, no. 1, article 168781401882537, 2019.

[23] B.-W. Moon, J.-H. Park, S.-K. Lee, J. Kim, T. Kim, and K.-W. Min, "Performance evaluation of a transmission tower by substructure test," *Journal of Constructional Steel Research*, vol. 65, no. 1, pp. 1–11, 2009.

[24] R. H. Yin, D. L. Li, G. L. Liu et al., "Seismic damage and analysis of power transmission towers," *World Information on Earthquake Engineering*, vol. 21, no. 1, pp. 51–54, 2005.

[25] H.-N. Li, W.-L. Shi, G.-X. Wang, and L.-G. Jia, "Simplified models and experimental verification for coupled transmission tower-line system to seismic excitations," *Journal of Sound and Vibration*, vol. 286, no. 3, pp. 569–585, 2005.

[26] Y. Liu and A. P. Tang, "The present research situation and earthquake damage defensive measures of the transmission lines," in *Proceedings of the 15th World Conference of Earthquake Engineering*, pp. 24–28, Lisbon, Portugal, September 2012.

[27] F. Wang, S. Q. Li, and J. Yang, "Response analysis of cathead transmission tower seismic performance based on Open Sees," in *Proceedings of the 2014 5th International Conference on Intelligent Systems Design and Engineering Applications*, Hunan, China, 2014.

[28] L. Tian, H. Li, and G. Liu, "Seismic response of power transmission tower-line system subjected to spatially varying ground motions," *Mathematical Problems in Engineering*, vol. 2010, Article ID 587317, 20 pages, 2010.

[29] K. S. Luo, Y. Wang, Y. T. Zhang et al., "Numerical simulation of section subway tunnel under surface explosion," *Journal of PLA University of Science and Technology*, vol. 8, no. 6, pp. 674–679, 2007.

[30] S. Yu and H. Ding, "Research on controlled blasting technology of large span and adjacent tunnel under passing high voltage tower," *Technology of Highway and Transport*, vol. 3, pp. 125–129, 2013, in Chinese.

[31] H. Yu, X. Yan, A. Bobet, Y. Yuan, G. Xu, and Q. Su, "Multi-point shaking table test of a long tunnel subjected to non-uniform seismic loadings," *Bulletin of Earthquake Engineering*, vol. 16, no. 2, pp. 1041–1059, 2018.

[32] H. Yu, Y. Yuan, C. Li, X. Yan, and J. Yuan, "Multi-point shaking table test for long tunnels subjected to non-uniform seismic loadings—part I: theory and validation," *Soil Dynamics and Earthquake Engineering*, vol. 108, pp. 177–186, 2018.

[33] H. Yu, Y. Yuan, G. Xu, Q. Su, X. Yan, and C. Li, "Multi-point shaking table test for long tunnels subjected to non-uniform seismic loadings—part II: application to the HZM immersed tunnel," *Soil Dynamics and Earthquake Engineering*, vol. 108, pp. 187–195, 2018.

[34] S. R. Zhang, X. C. Feng, and M. Yu, "Analysis of Approaching influence of shield double-line tunnel passing under communication tower," *Railway Way Standard Design*, vol. 60, no. 6, pp. 100–105, 2016, in Chinese.

[35] R. J. Mair, D. I. Harris, J. P. Love, D. Blakey, and C. Kettle, "Compensation grouting to limit settlements during

tunnelling at Waterloo Station, London," in *Tunnelling'94*, Springer, Boston, MA, USA, 1994.

[36] X. M. Guan, "Blasting vibration characteristics monitoring of tunnel under-passing hillside buildings in short-distance," *Rock and Soil Mechanics*, vol. 35, no. 7, 2014.

[37] F. Albermani, S. Kitipornchai, and R. W. K. Chan, "Failure analysis of transmission towers," *Engineering Failure Analysis*, vol. 16, no. 6, pp. 1922–1928, 2009.

[38] T. Li, G. Xia, Q. Bing, H. Li, and P. Zhang, "Influence of spatial variation of ground motions on dynamic responses of supporting towers of overhead electricity transmission systems: an experimental study," *Engineering Structures*, vol. 128, pp. 67–81, 2016.

[39] China Architecture & Building Press, *Code for Design of Steel Structures (GB 50017-2003)*, China Architecture & Building Press, Beijing, China, 2003, in Chinese.

[40] J. X. Lai, J. L. Qiu, H. B. Fan et al., "Fiber bragg grating sensors-based in-situ monitoring and safety assessment of loess tunnel," *Journal of Sensors*, vol. 2016, Article ID 8658290, 10 pages, 2016.

[41] B. Giorgio, "Blasting-induced vibration in tunnelling," *Tunnelling and Underground Space Technology*, vol. 9, no. 2, pp. 175–187, 1994.

[42] Y. Jiang, X. Zhang, and T. Taniguchi, "Quantitative condition inspection and assessment of tunnel lining," *Automation in Construction*, vol. 102, pp. 258–269, 2019.

[43] X. H. Li, Y. Long, and C. Ji, "Study on the vibration effect on operation subway induced by blasting of an adjacent cross tunnel and the reducing vibration techniques," *Journal of Vibroengineering*, vol. 15, no. 3, pp. 1454–1462, 2013.

[44] Z. J. Zhou, C. N. Ren, G. J. Xu, H. C. Zhan, and T. Liu, "Dynamic failure mode and dynamic response of high slope using shaking table test," *Shock and vibration*, vol. 2019, Article ID 4802740, 19 pages, 2019.

[45] Z. Q. Zhang, H. Zhang, Y. Tan, and H. Yang, "Natural wind utilization in the vertical shaft of a super-long highway tunnel and its energy saving effect," *Building and Environment*, vol. 145, pp. 140–152, 2018.

[46] X. F. Deng, J. B. Zhu, S. G. Chen, Z. Y. Zhao, Y. X. Zhou, and J. Zhao, "Numerical study on tunnel damage subject to blast-induced shock wave in jointed rock masses," *Tunnelling and Underground Space Technology*, vol. 43, pp. 88–100, 2014.

[47] K. Shitang, Xu. Lu, and J. G. Yao, "Sensitivity analysis and estimation method of natural frequency for large cooling tower based on field measurement," *Thin-Walled Structures*, vol. 127, pp. 809–821, 2018.

[48] M. Y. Park, S. Kim, I. Paek, and C. Cui, "Frequency analysis of a tower-cable coupled system," *Journal of Mechanical Science and Technology*, vol. 27, no. 6, pp. 1731–1737, 2013.

[49] H.-B. Zhao, Y. Long, X.-H. Li, and L. Lu, "Experimental and numerical investigation of the effect of blast-induced vibration from adjacent tunnel on existing tunnel," *KSCE Journal of Civil Engineering*, vol. 20, no. 1, pp. 431–439, 2016.

[50] Z. J. Zhou, S. S. Zhu, X. Kong, J. Lei, and T. Liu, "Optimization analysis of settlement parameters for post-grouting piles in loess area of Shaanxi, China," *Advances in Civil Engineering*, vol. 2019, Article ID 7085104, 11 pages, 2019.

[51] J. X. Lai, K. Wang, J. L. Qiu, F. Niu, J. Wang, and J. Chen, "Vibration response characteristics of the cross tunnel structure," *Shock and Vibration*, vol. 2016, Article ID 9524206, 16 pages, 2016.

[52] Y. W. Zhang, Z. P. Song, X. L. Weng, and Y. Xie, "A new soil-water characteristic curve model for unsaturated loess based on wetting-induced pore deformation," *Geofluids*, vol. 2019, Article ID 5261985, 14 pages, 2019.

[53] H.-S. Park, B. H. Choi, J. J. Kim, and T.-H. Lee, "Seismic performance evaluation of high voltage transmission towers in South Korea," *KSCE Journal of Civil Engineering*, vol. 20, no. 6, pp. 2499–2505, 2016.

[54] J. B. Wang, W. W. Li, and Z. P. Song, "Development and implementation of new triangular finite element based on MGE theory for bi-material analysis," *Results in Physics*, vol. 13, article 102231, 2019.

[55] Q. X. Yan, H. Chen, W. Chen, J. Zhang, S. Ma, and X. Huang, "Dynamic characteristic and fatigue accumulative damage of a cross shield tunnel structure under vibration load," *Shock and vibration*, vol. 2018, Article ID 9525680, 13 pages, 2018.

[56] S. J. Wang, Z. Y. Wu, and W. L. Dong, *Elastic Wave Test of Rock Mass in Hydropower Project*, Science Press, Beijing, China, 1982.

[57] J Dai, *Rock Dynamics and Blasting Theory*, Metallurgical Industry Press, Beijing, China, 2002, in Chinese.

[58] J.-H. Shin, H.-G. Moon, and S.-E. Chae, "Effect of blast-induced vibration on existing tunnels in soft rocks," *Tunnelling and Underground Space Technology*, vol. 26, no. 1, pp. 51–61, 2011.

[59] J. A. Sharpe, "The production of elastic waves by explosion pressures. I. Theory and empirical field observations," *Geophysics*, vol. 7, no. 2, pp. 144–154, 1942.

[60] X. B. Yue, Y. L. Xie, H. G. Zhang et al., "Study on geotechnical characteristics of marine soil at Hongkong-Zhuhai-Macao tunnel," *Marine Georesources and Geotechnology*, 2019.

[61] L. M. Duan, Y. H. Zhang, and J. X. Lai, "Influence of ground temperature on shotcrete-to-rock adhesion in tunnels," *Advances in Materials Science and Engineering*, vol. 37, no. 8, pp. 1–12, 2019.

[62] P. F. Li, F. Wang, L. F. Fan, H. D. Wang, and H. D. Ma, "Analytical scrutiny of loosening pressure on deep twin-tunnels in rock formations," *Tunnelling and Underground Space Technology*, vol. 83, pp. 373–380, 2019.